Int. J. Heat Mass Transfer. Vol. 9, pp. 1047–1060. Pergamon Press 1966. Printed in Great Britain

AN INVESTIGATION INTO TURBULENT SUBMERGED JETS OVER A WIDE TEMPERATURE RANGE†

G. N. ABRAMOVICH, V. I. BAKULEV, V. A. GOLUBEV and G. G. SMOLIN
Moscow

(*Received* 8 *July* 1965)

Аннотация—Работа посвящена теоретическому и экспериментальному исследованию затопленных неизотермических турбулентных струй в диапазоне начальных температур от 50–100°K до 20×10^3 °K.

NOMENCLATURE

$x, y,$ independent variables;
$\eta, \varphi,$ new independent variables, derivatives of x and y;
$u,$ velocity component parallel to the axis x;
$v,$ velocity component parallel to the axis y;
$\rho,$ density;
$V,$ specific volume;
$i,$ enthalpy;
$T,$ temperature;
$P,$ pressure;
$Z,$ velocity function;
$F,$ current density function;
$\vartheta,$ density function;
$\theta,$ specific volume function;
$\varepsilon, \tau,$ enthalpy function;
$b_*,$ relative width of a boundary layer of a jet;
$a,$ empirical constant;
$Re,$ Reynolds number;
$Pr_t,$ turbulent Prandtl number;
$R_0,$ nozzle radius;
$\delta,$ coefficient (for a flat-parallel flow $\delta = 0$; for an axisymmetric flow $\delta = 1$);
$\alpha, D, A, B, C,$ coefficients dependent on the kind of a working substance and temperature range;
$J, j,$ definite integrals;
$\tilde{a},$ coefficients } are used for solv-
$\tilde{\varphi},$ functions } ing the equations;
$\varepsilon_{exp},$ experimental coefficient of radiation;
$\varepsilon_{theor},$ theoretical coefficient of radiation;
$H_\beta,$ line of atomic hydrogen.

Subscripts

$O,$ initial parameters of a jet;
$H,$ parameters of a surrounding medium;
$m,$ parameters on the jet axis;
$b,$ jet boundary;
$cr,$ critical parameters.

A bar over a symbol denotes a parameter averaged over time.

STATEMENT OF PROBLEM

TWO REGIONS of isobaric jet flows are considered: cold (or heavy) jets with a low initial temperature (50–100°K) spreading in a medium with an increased temperature (300–400°K) and hot (or light) jets with a very high initial temperature ($\sim 20 \times 10^3$ °K), spreading in a medium with a moderate temperature (~ 300°K). The initial working substance of a jet and the

† The present work was reported by the authors at the Second All-Union Congress of Theoretical and Applied Mechanics.

surrounding medium has the same chemical composition.

A heavy jet with the initial liquid parameters spreads in a gaseous medium at a supercritical thermodynamic pressure for a given working substance. In this case the working substance of a jet with non-isothermal mixing is not subjected to phase conversions and the flow pattern is qualitatively the same as that in purely gaseous jets [1].

In a boundary layer of both the heavy and light jets a change takes place not only of the temperature of the working substance but also of its heat capacity. Therefore, when stating such problems it is advisable to use the enthalpy as the measure of the energy content of a gas.

The application of an ordinary equation of state for studying the behaviour of heavy jets at a thermodynamic pressure higher than the critical one may lead to essential errors. Therefore, in order to calculate such jets, it is proposed to use the dependence approximating the equation of state [2] which allows for the peculiarities of the phenomena occurring in a gas:

$$\bar{i} = A\overline{V} + B + \frac{C}{\overline{V}} + \frac{D}{\overline{V}^2}, \qquad (1)$$

where $\bar{i}$ is the averaged enthalpy; $\overline{V}$ is the averaged specific volume; A, B, C and D are the coefficients dependent on the kind of working substance and its pressure.

In a boundary layer of a hot jet with a high initial temperature physico-chemical conversions take place (dissociation, ionization and recombination). This leads to the fact that even a monoatomic gas becomes multicomponent, and its gas constant and heat capacity (provided that thermodynamic processes are in equilibrium) vary substantially with temperature. For the calculation of such jets, it is proposed to use the dependence of gas enthalpy on density, obtained from the thermodynamic calculation and approximated by the expression [3]:

$$\bar{i} = \frac{A}{\overline{\rho}^{\alpha}} = A\overline{V}^{\alpha} \qquad (2)$$

where A and α are the quantities dependent on the kind of working substance employed and the range of the temperature considered.

The use of this relation allows the physico-chemical conversions occurring in a gas to be taken into consideration and at the same time considerably simplifies the calculation.

The scheme proposed by Tomlin [1] is used for solving the boundary-layer problems of cold and hot jets. The jet is divided into two portions: initial and main. The flow in the initial portion of the axisymmetric jet according to the Tolmin scheme is conditionally replaced by an infinite flat-parallel free boundary layer with the origin of the co-ordinates at the edge of a nozzle.

The flow in the main portion is replaced by a source, i.e. by an axisymmetric jet flowing from an infinitely small hole with the origin of the co-ordinates at the source pole. The matching of the initial and main portions of the jet is made over the transition section, on whose axis the velocity u_m is equal to the initial jet velocity u_0.

The change of the parameters in the cross-section of the initial and main portions of a jet is determined by the averaged differential equations for a free boundary layer.

$$\overline{\rho v}\frac{\partial \bar{u}}{\partial y} + \overline{\rho u}\frac{\partial \bar{u}}{\partial x} = \pm \frac{1}{y^{\delta}} c^2 x^2 \times \frac{\partial}{\partial y}\left[y^{\delta}\bar{\rho}\left(\frac{\partial \bar{u}}{\partial y}\right)^2\right] \qquad (3)$$

Discontinuity equation:

$$\frac{\partial \overline{\rho u}}{\partial x} + \frac{\partial \overline{\rho v}}{\partial y} + \delta\frac{\overline{\rho v}}{y} = 0 \qquad (4)$$

Energy equation:

$$\overline{\rho v}\frac{\partial \bar{i}}{\partial y} + \overline{\rho u}\frac{\partial \bar{i}}{\partial x} = \pm \frac{1}{y^{\delta}}\frac{C^2 x^2}{Pr_t} \times \frac{\partial}{\partial y}\left[y^{\delta}\bar{\rho}\frac{\partial \bar{u}}{\partial y}\frac{\partial \bar{i}}{\partial y}\right] \qquad (5)$$

In these equations $\bar{u}$, $\bar{v}$ are the components of the averaged velocity along the axis x and y,

respectively; δ is the coefficient (for a flat-parallel flow $\delta = 0$ and for an axisymmetric flow $\delta = 1$). The turbulent friction in the motion equation and the heat flux in the energy equation are presented on the basis of the free turbulence Prandtl theory since the use of the Taylor turbulence theory for calculating compressible gas jets becomes incorrect [4].

As the experiments show, the temperature profiles in non-isothermal jets are always more full than the velocity profiles. The comparison of these profiles shows that the turbulent Prandtl number is within $1 > Pr_t \geqslant 0{\cdot}5$. The dependence approximating the equation of state for cold and hot jets may be written in a general form:

$$\bar{i} = A\bar{V}^{\alpha} + B + \frac{C}{\bar{V}} + \frac{D}{\bar{V}^2} \tag{6}$$

In order to determine the velocity on the axis of the source u_m and the co-ordinate of the considered cross-section x it is possible to use:

(a) the equation of the constancy of excess momentum,

$$2\pi \int_0^{y_b} \overline{\rho u}(\bar{u} - u_H) y \, dy = \rho_0 u_0 (u_0 - u_H)\pi R_0^2; \tag{7}$$

(b) the equation of the constancy of excess heat content,

$$2\pi \int_0^{y_b} \overline{\rho u}(\bar{i} - i_H) y \, dy = \rho_0 u_0 (i_0 - i_H)\pi R_0^2. \tag{8}$$

In these expressions R_0 is the initial radius of the jet; y_b is the co-ordinate of the boundary of the jet; the initial parameters of the jet are designated through subscript 0; H are the parameters of the surrounding medium.

In solving the problem the heat and dynamic widths of the jet are assumed to be the same.

PROBLEM OF INFINITE FLAT-PARALLEL BOUNDARY LAYER

The internal and external boundaries of a boundary layer are assumed to be rectilinear and the dimensionless values of the same parameters in different cross-sections to be affine.

If

$$x \text{ and } \eta = \frac{(y/ax) - (y_2/ax)}{b_*} \tag{9}$$

are taken as independent variables where $a = \sqrt[3]{(2c^2)}$ is the empirical constant; $b_* = (y_1/ax) - (y_2/ax)$ is the relative width of a boundary layer; y_1 is the co-ordinate of the internal boundary; y_2 is the co-ordinate of the external boundary, then the dimensionless functions of the parameters

$$\frac{\bar{u}}{u_0} = Z(\eta); \quad \frac{\overline{\rho u}}{\rho_0 u_0} = F'(\eta); \quad \frac{\bar{\rho}}{\rho_0} = \vartheta(\eta);$$
$$\frac{\bar{V}}{V_0} = \theta(\eta); \quad \frac{\bar{i}}{i_0} = \tau(\eta) \tag{10}$$

will depend only upon the variable η.

Before transforming the differential boundary-layer equations, with the help of the free turbulent Prandtl theory [1] we shall write down the equation relating the current density $\overline{\rho u}$ to the velocity $\bar{u}$:

$$\overline{\rho u} = \bar{\rho}\bar{u} + \overline{\rho' u'} = \bar{\rho}\bar{u} + \frac{1}{Pr_t} c^2 x^2 \frac{\partial \bar{\rho}}{\partial y}\frac{\partial \bar{u}}{\partial y}. \tag{11}$$

We shall transform the equation of motion (3) and also equations (4) and (11) with the help of functions (10) into a new system of co-ordinates (9), obtaining the differential equation:

$$L(Z) = Z'''(\eta) - \frac{3\theta'}{2\theta} Z''(\eta) - \left[\frac{1}{2Pr_t} b_* \frac{\theta'}{\theta} + \left\{\tfrac{1}{2}\frac{\theta''}{\theta} - \left(\frac{\theta'}{\theta}\right)^2\right\}\right] Z'(\eta) + b_*^3 Z(\eta) = 0; \tag{12}$$

with the boundary conditions at:

$$\eta = 1; \quad \bar{u} = u_0, \quad Z(1) = 1;$$
$$\frac{\partial \bar{u}}{\partial y} = 0, \quad Z'(1) = 0; \quad \overline{\rho v} = 0;$$
$$Z''(1) = -\frac{y_1}{ax} b_*^2; \tag{13}$$

at

$$\eta = 0; \qquad \bar{u} = u_H = 0, \qquad Z(0) = 0;$$

$$\frac{\partial \bar{u}}{\partial y} = 0, \qquad Z'(0) = 0;$$

where $y_1/ax = \varphi_1$.

In equations (12)

$$\frac{\theta'}{\theta} \quad \text{and} \quad \tfrac{1}{2}\frac{\theta''}{\theta} - \left(\frac{\theta'}{\theta}\right)^2 = \sigma(\eta)$$

are functions of η, whose form may be determined from the solution of the energy equation.

The solutions of the equation of motion (12) simultaneously with its boundary conditions (13) may be found in a general form by the Galerkin method [2]:

$$Z_n = \sum_1^n \tilde{a}_k \tilde{\varphi}_k \qquad (k = 1, 2, 3, \ldots n). \tag{14}$$

Let us write the solution of equation (12) in the expanded form:

$$Z_n = \tilde{a}_1(2\eta^3 - 3\eta^2) + \tilde{a}_2(1-\eta)^2\eta^2 + \tilde{a}_3(1-\eta)^2\eta^3 + \ldots + \tilde{a}_k(1-\eta)^2\eta^k. \tag{14'}$$

The system of functions $\tilde{\varphi}_k$ is so chosen that at $\tilde{a}_1 = -1$ and for any values of $\tilde{a}_2, \tilde{a}_3, \ldots \tilde{a}_k$ it satisfies four out of the five boundary conditions of equations (13).

Consider the solution to a second approximation which has the form:

$$Z_2 = -(2\eta^3 - 3\eta^2) + \tilde{a}_2(1-\eta)^2\eta^2. \tag{15}$$

To a second approximation $\tilde{a}_2$, b_* and φ_1 will be unknown. Using the Galerkin method, we shall set two equations for determining the unknowns:

$$\int_0^1 L(Z_2)\tilde{\varphi}_1 \, d\eta = 0; \qquad \int_0^1 L(Z_2)\tilde{\varphi}_2 \, d\eta = 0 \tag{16}$$

and as the third equation we shall take the boundary condition

$$Z_2''(1) = -\varphi_1 b_*^2. \tag{17}$$

To a second approximation the solution is reduced to determining the unknowns $\tilde{a}_2$, b_* and φ_1 from equations (16) and (17) which contain the definite integrals:

$$J_k = \int_0^1 \frac{\theta'}{\theta}\eta^k \, d\eta; \qquad j_k = \int_0^1 \sigma(\eta)\eta^k \, d\eta \qquad (k = 2, 3, 4, \ldots) \tag{18}$$

The integrands of the functions of (18) may be determined from the solution of the energy equation.

Similarly, the system of the equations for any value of k may be found by the Galerkin method.

For $k > 3$ it becomes difficult to determine the unknowns since finally we are to deal with the system of $(k+1)$ non-linear algebraic equations.

Let us pass to the solution of energy equation (5) simultaneously with (6). We transform energy equation (5) simultaneously with equations (3), (4), (11) with the help of functions (10) into the system of co-ordinates (9). Thus, we have the energy equation in the form:

$$-k_1\frac{\theta'}{\theta} + k_2\frac{Z''}{Z'} + \frac{\tau''}{\tau'} = 0; \tag{19}$$

with the boundary conditions at:

$$\eta = 1; \qquad Z(1) = 1, \qquad \theta(1) = 1, \qquad \tau(1) = 1;$$

at (20)

$$\eta = 0; \qquad Z(0) = 0, \qquad \theta(0) = V_H/V_0, \qquad \tau(0) = i_H/i_0$$

where

$$k_1 = 1 - Pr_t, \qquad k_2 = 1 - 2Pr_t.$$

We shall now present equation (6) in a dimensionless form:

$$i_0\tau = AV_0^{\alpha}\theta^{\alpha} + B + (C/V_0\theta) + (D/V_0^2\theta^2) = f(\theta). \tag{21}$$

The energy equation (19) is solved simultaneously with (21) as follows:

$$\int \frac{f'(\theta)}{\theta^{k_1}} d\theta = C_1 \int (Z')^{-k_2} d\eta + C_2. \tag{22}$$

The integration constants C_1 and C_2 are determined by the boundary conditions (20).

The parameters of the initial portion of a jet are calculated by the method of successive approximation, using the system of equations (16), (17) and (22) with an arbitrary value of the turbulent Prandtl number Pr_t. For $Pr_t = 0{\cdot}5$ the calculation is greatly simplified since in this case $k_2 = 0$.

The solution of the problem on an infinite flat parallel boundary layer for a hot jet was obtained in the series for the turbulent Prandtl number $Pr_t = 0{\cdot}5$ [3, 4].

PROBLEM ON A BOUNDARY LAYER OF AN AXISYMMETRIC TURBULENT SOURCE

The investigations of the initial portion of non-isothermal jets [2–4] have shown that the profiles of the same parameters obtained for different ratios ρ_0/ρ_H in the dimensionless co-ordinates are not similar.

In the main portion of the jet the relation of the density at the axis to that of the surrounding medium ρ_m/ρ_H varies along the length and, consequently, it may be expected that the profiles of the same parameters depending on ρ_m/ρ_H are also not similar as in the case of the initial jet portion. It is therefore proposed to solve the problem by the method of local similarity.

The main portion of the length is divided into short sections Δx. On such a section Δx the flow is assumed to be automodel [5] and the profiles to be affine, i.e. the density ρ_m along the section Δx will be considered to be approximately constant. Averaged equations (3) to (5) for the axisymmetric quasi-stationary flow and equation (6) are used to determine the parameters for each of such sections.

The velocity u_m on the axis and the co-ordinate x of the cross-section under consideration were determined with the help of the equations for constancy of excess momentum (7) and for heat content (8), respectively.

Let us take as new independent variables

$$x \text{ and } \eta = \frac{\varphi}{b_*} \tag{23}$$

where $\varphi = y/ax$, $b_* = y_b/ax$ is the relative half-width of the jet and $a = \sqrt[3]{c^2}$ is an empirical constant.

The dimensionless functions of the main parameters

$$\frac{\bar{u}}{u_m} = z(\eta); \quad \frac{\overline{\rho u}}{\rho_m u_m} = \frac{F'(\eta)}{\eta}; \quad \frac{\bar{\rho}}{\rho_m} = \vartheta(\eta);$$
$$\frac{\bar{V}}{V_m} = \theta(\eta); \quad \frac{\bar{i}}{i_m} = \tau(\eta) \tag{24}$$

on the section Δx will depend only upon the variable η. Here the symbol m denotes parameters at the axis.

If we pass to a new system of co-ordinates (23) in the equation of motion (3) and transform it simultaneously with equations (4), (7), (8) and (11), with the help of functions (24), then the equation of motion will be obtained:

$$L(Z) = Z^3 b_*^3 + \frac{\theta'}{\theta}(Z')^2 Z - 2Z''Z'Z + (Z')^3$$
$$- (Z')^2 Z \frac{1}{\eta} - a \frac{1}{Pr_t} \frac{\theta'}{\theta} Z' Z^2 b_* = 0; \tag{25}$$

with the boundary conditions at:

$$\eta = 0; \quad \bar{u} = u_m, \quad Z(0) = 1;$$
$$\bar{\rho}\bar{v} = 0, \quad Z'(0) = 0;$$
at
$$\eta = 1; \quad \bar{u} = u_H = 0, \quad Z(1) = 0. \tag{26}$$

The inspection of equation (25) at the boundaries shows the following.

At $\eta = 0$ the equality $b_*^3 = 2z'(0)z''(0)$ should be satisfied but since $b_* \neq 0$,

$$Z''(0) \to \infty. \tag{27}$$

At $\eta = 1$ the solution of equation (25) will satisfy the boundary condition if

$$Z'(1) = 0. \tag{28}$$

The solution of equation (25) should satisfy two additional conditions which are obtained

by analysing the equation of motion (25) at the boundaries.

We shall seek for the solution of the equation of motion (25) simultaneously with the main (26) and secondary (27), (28) boundary conditions by the Galerkin method:

$$Z_n = \sum_0^n \tilde{a}_k \tilde{\varphi}_k \qquad (k = 0, 1, 2, \ldots n). \tag{29}$$

The system of the functions $\tilde{\varphi}_k$ is chosen so that for the preliminary chosen values of the coefficients $\tilde{a}_0 = 1$ and $\tilde{a}_1 = 1$ and at the arbitrary values of all the subsequent coefficients $\tilde{a}_2$, $\tilde{a}_3$ ... $\tilde{a}_k$ it would automatically satisfy the boundary conditions (26) to (28).

We shall write the solution of equation (25) in the expanded form:

$$Z_n = 1 + (3\eta^2 - 4\eta^{\frac{3}{2}}) + \tilde{a}_2(1-\eta)^2\eta^{\frac{3}{2}} + \tilde{a}_3(1-\eta)^2\eta^3 + \ldots + \tilde{a}_k(1-\eta)^2\eta^{\frac{3(k-1)}{2}} \tag{30}$$

Consider the solution to a second approximation, i.e. at $k = 2$

$$z_2 = 1 + (3\eta^2 - 4\eta^{\frac{3}{2}}) + \tilde{a}_2(1-\eta)^2\eta^{\frac{3}{2}} \tag{31}$$

For the second approximation it is necessary to find two unknowns $\tilde{a}_2$ and b_*, for the determination of which two equations are set up according to the Galerkin method:

$$\int_0^1 L(Z_2)\tilde{\varphi}_1 \, d\eta = 0; \qquad \int_0^1 L(Z_2)\tilde{\varphi}_2 \, d\eta = 0. \tag{32}$$

Equation (32) contains the integrals

$$\int_0^1 \frac{\theta'}{\theta}\eta^k \, d\eta \qquad (k = 1, \tfrac{3}{2}, 2, \tfrac{5}{2}, 3 \ldots) \tag{33}$$

whose values may be determined by the method of successive approximations from equations (32), (21) and the energy equation.

The system of the equations for $k > 2$ may be set up by the same method, but it is rather difficult to operate with such a system since eventually a non-linear system of equations is obtained.

Energy equation (5) simultaneously with equations (3), (4), (7), (8), (11) is transformed into the system of the co-ordinates (23) by means of the functions (24).

We obtain the energy equation:

$$Pr_t \frac{Z'}{Z} = \frac{\varepsilon'}{\varepsilon}; \tag{34}$$

with the boundary conditions at:

$$\text{at} \quad \begin{aligned} &\eta = 0; \quad Z(0) = 1, \quad \varepsilon(0) = 1; \\ &\eta = 1; \quad Z(1) = 0, \quad \varepsilon(1) = 0; \end{aligned} \tag{35}$$

where

$$\varepsilon = \frac{i - i_H}{i_m - i_H}.$$

The solution of energy equation (34) simultaneously with the boundary conditions (35) is of the form:

$$\varepsilon = Z^{Pr_t}. \tag{36}$$

The parameter profiles in the cross-section under consideration are determined by the method of the successive approximations.

When calculating the cross-section chosen ρ_m is the unknown quantity, whose value is taken constant in this cross-section.

To a first approximation the specific-volume profile is taken along the cross-section thus:

$$\theta = \left(\frac{V_H}{V_m}\right)^\eta = \theta_H^\eta \tag{37}$$

Then, the function entering into the integrals of expression (33) will be constant

$$\frac{\theta'}{\theta} = \ln \theta_H = \text{const}. \tag{38}$$

Solving the system of equations (32) we find the velocity profile and the relative width of the cross-section considered, and the enthalpy profile is determined from equation (36).

The exact value of the specific-volume profile θ and the function θ'/θ is determined by approximating equation (21). Thus, by the method of successive approximations it is possible to obtain the profiles of the main parameters in

this cross-section, and then to find its co-ordinate x and the relative velocity u_m on the cross-section axis.

The cross-section co-ordinate may be found by means of the equation of the constancy of excess heat content. For this purpose equation (8) simultaneously with equations (4), (11) is transformed into the system of the co-ordinates (23) by means of the functions (24). The relative co-ordinate of the cross-section under consideration [5] is simply determined from the equation obtained

$$\frac{ax}{R_0} = \frac{0{\cdot}707\sqrt{\left(\int_0^1 F'Z\,d\eta\right)}\sqrt{(\rho_0/\rho_m)}}{\frac{i_m - i_H}{i_0 - i_H} b_* \int_0^1 F'\varepsilon\,d\eta} \qquad (39)$$

Similarly it is possible to transform equation (7) for the constancy of excess momentum simultaneously with equations (4) and (11).

The equation for the determination of the relative velocity at the axis of the cross-section considered is obtained:

$$\frac{u_m}{u_0} = \frac{0{\cdot}707\sqrt{(\rho_0/\rho_m)}}{(ax/R_0)b_*\sqrt{\left(\int_0^1 F'Z\,d\eta\right)}}. \qquad (40)$$

The main portion of an axisymmetric submerged jet, non-automodel along the length with an arbitrary value of the Prandtl number Pr_t, may be calculated by the method proposed. The problem of the main portion of a hot axisymmetric jet was also solved by using the Taylor model.

RESULTS OF THE EXPERIMENTAL STUDIES OF COLD AND HOT JETS

Axisymmetric cold jets were experimentally studied on the apparatus where a high-pressure barochamber served as a working section.

The runs were carried out on a nitrogen jet with the properties of a liquid which spread to a medium of gaseous nitrogen at a supercritical thermodynamic pressure. The liquid nitrogen jet had an initial temperature $T_0 = 80°$–$90°$K and spread in a gaseous nitrogen medium at a chamber pressure of $P_{ch} = 40$ at (critical nitrogen parameters: $T_{cr} = 126°$K; $P_{cr} = 34{\cdot}6$ at).

The nozzle diameter was 5,3 and 1·12 mm. The nitrogen jet velocity varied over the range of $u_0 = 20$–50 m/s. The Reynolds numbers calculated at the outlet cross-section of the nozzle were $Re = (1{\cdot}7$–$5{\cdot}8) \times 10^5$, respectively.

The runs were conducted in two ranges of temperatures of the surrounding medium: $T_H = 250$–$300°$K and $T_H = 370$–$420°$K. The co-current wake flow velocity did not exceed 0·3 m/s, and therefore the jet may be considered to be submerged with a sufficient degree of accuracy.

The dynamic head in the cross-sections of the cold nitrogen jet was measured by the pressure head, whose indications were recorded on two differential manometers: a mercury one for measuring small pressure drops and an encased manometer for measuring large pressure drops. The jet cross-section temperature was measured by a copper–constantan thermocouple.

The hot jets were experimentally studied on an open a.c. plasmatron with water arc stabilization. Water vapour served as a working substance of the jet. The value of the arc current varied from 200 to 1300 A, which corresponded to the initial jet temperature $T_0 = (15$–$20) \times 10^3°$K. The jet discharged from the nozzle, whose diameters varied from 2·3 to 16 mm in various runs, with the initial velocity $u_0 = 600$–4400 m/s (a maximum value of the Mach number did not exceed 0·6). The Reynolds numbers based on the outlet cross-section of a nozzle were within $Re = (1{\cdot}5$–$6) \times 10^4$. The water vapour jet spread in the stationary surrounding air at $T_H = 280$–$295°$K. The spectrographic method was used for determining the temperature field in the cross-sections of the hot jet. The spectrum was photographed on the spectrograph ИСП-28 together with the spectrum of a standard reference tungsten lamp СИ-14. Comparing the density of the blackening of the test spectrum with that of the standard reference

lamp, whose energy is known, it is possible to obtain the distribution of the integral radiation intensity along the jet radius. The solution of the Abel equation makes it possible to pass from the integral radiation intensity to a radial distribution of the radiation coefficients ε_{exp}.

The relative radiation coefficients ε_{theor} are determined on the basis of the thermodynamic calculation depending on a temperature. Comparing the values of the coefficients ε_{exp} and ε_{theor} it is possible to obtain a temperature distribution along the jet radius. The temperatures in the cross-sections of the hot jet were measured from the line of atomic hydrogen H_β. The above method of measurement of temperatures gives an unsatisfactory reproducibility of the results due to the difficulty of maintaining the set operating conditions from run to run.

The photographic express method which is a variety of the spectrographic method of the relative Lorentz intensities is used for determining the temperature field in a hot jet. When measuring the temperatures by this method the whole jet is photographed in monochromatic light by a camera equipped with a set of light filters (ЖС-16, ЖС-17, СС-5 and СЗС-18) which selected a narrow region of the spectrum corresponding to the wave length of the line H_β.

The discrepancies in the temperatures measured along the jet radius by these methods did not exceed 7 per cent.

The high-speed camera СФР-2 was used to measure directly the velocity in a hot jet. This method of determination of the velocity is based on the existence in a jet of zones of higher luminosity. The displacement of these zones is recorded in continuous scanning.

The special experiments using a slit diaphragm and the introduction of mechanical disturbances into a jet have shown that the available luminosity fluctuations in luminous zones practically spread over the whole jet volume, and the velocities of their displacement recorded by a high-speed camera are close to the jet velocity. The presence of the zones with different luminosity in the jet volume is apparently explained by the changes in the electric contact of the jet with the annular electrode at the outlet of a plasmatron. The frequency of oscillations of the jet luminosity is not periodic and we failed to find the effect of any factor upon the frequency of these oscillations. Its value varied on the average within 7000–10000 cps.

During the filming the slit diaphragm of the chamber was positioned along the jet axis. By moving the diaphragm parallel to the jet axis it is possible to observe the changes in the velocity along the jet radius. We had to assume that the zone of higher luminosity had the greatest brightness on the axis and which uniformly decreased to the jet periphery. Thus, the velocity of the brightest part of the disturbance zone is recorded at any position of the diaphragm slit; and the remaining less bright layers of the zone are rendered invisible.

The assumption made about the distribution of brightness along the jet radius is verified by the experimentally obtained distribution of the radiation intensity along the jet radius.

From the observation of the change in the inclination angle of the brightest part of the trace of this disturbance along the jet length, it is easy to find the change in the velocity of the propagation of this disturbance. The error of the treatment of the experimental data did not exceed 6–10 per cent on the average.

Cold and hot jets were also studied qualitatively by means of the schlieren device ИАБ-451; in the experiments with hot jets the filming was done through the filter ЖС-17.

ANALYSIS OF EXPERIMENTAL RESULTS AND THEIR COMPARISON WITH THEORETICAL RESULTS

Figure 1 shows the schlieren photographs of cold, isothermal and hot jets. From the comparison of these photographs it is seen that the expansion angle of the jet and its width increase with the initial heating. This fact is also confirmed when for the same test we compare the profiles obtained in the cross-sections of the initial and

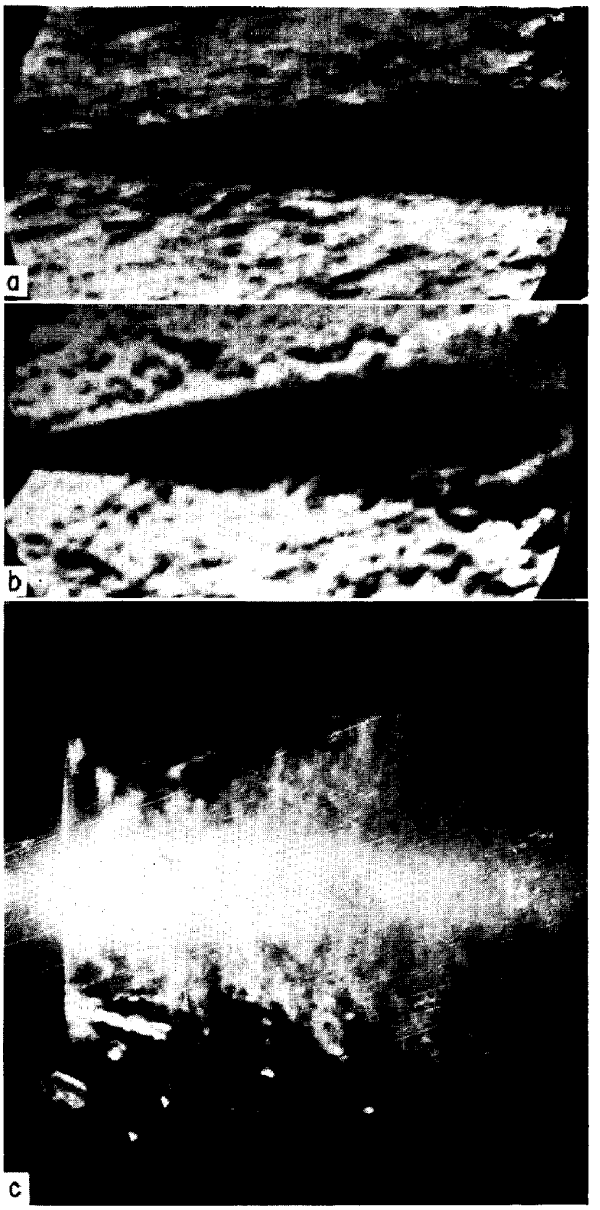

FIG. 1. Schlieren photographs of jets; (a) cold; (b) isothermal; (c) hot.

the main jet portions (see Figs. 2–6). The increase in the jet width with the initial heating agrees with the results of the theoretical calculations obtained in references [3, 4]. The broadening of the mixing zone leads to a decrease in the range of the jet and, consequently, to a decrease of the length of the initial portion (see Figs. 7, 8). From Fig. 8 it is seen that at the axis of the initial portion of a high temperature jet the enthalpy is not constant but somewhat drops. This apparently may be explained by the fact that some amount of energy of the jet is lost through radiation. A comparatively small temperature drop for large values of the latter follows from the fact that the degree of blackness of a plasma jet is small and equal to $(1–2) \times 10^{-3}$ [6]. From the shadowgraph photographs it is seen that the external boundaries of the cold and hot jets like the incompressible-liquid jets remain rectilinear. This confirms the assumption taken in the present calculation of a linear increase of the mixing path along the jet. The measured temperature profiles obtained in different cross-sections of the main portion of a cold jet are shown in Fig. 9. The analysis of these curves shows that the temperature profiles are not affine. This result agrees with the assumption on the non-similarity of flow along the length of the main portion of a jet. From the comparison of the profiles of temperature and velocity (Fig. 10) obtained on

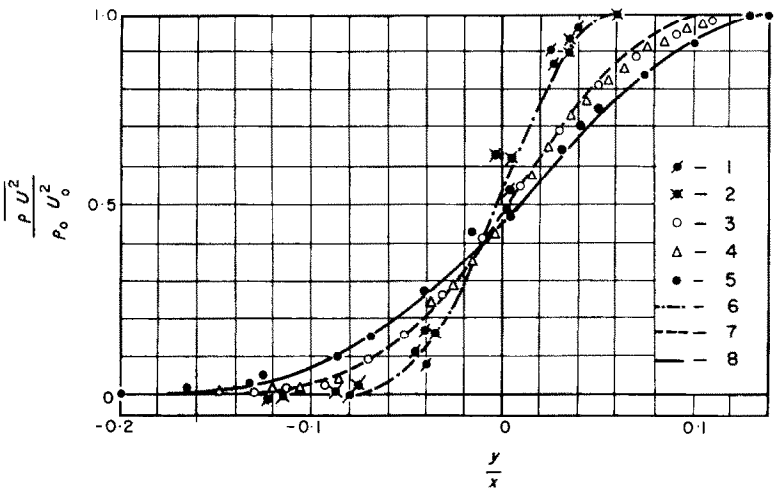

FIG. 2. Profiles of dynamic heads in a boundary layer of the initial portion of cold, isothermal and hot jets.

Experimental data

Cold jet:
1.—$x/R_0 = 10$; $T_H = 417°K$; $\rho_0/\rho_H = 20{\cdot}8$; $R_0 = 2{\cdot}5$ mm
2.—$x/R_0 = 16{\cdot}7$; $T_H = 360°K$; $\rho_0/\rho_H = 18{\cdot}8$; $R_0 = 1{\cdot}5$ mm

Isothermal jet:
3.—$x/R_0 = 2$; $R_0 = 25$ mm
4.—$x/R_0 = 4$; $R_0 = 25$ mm

Hot jet:
5.—$x/R_0 = 3{\cdot}33$; $\rho_0/\rho_H = 0{\cdot}067$; $R_0 = 15$ mm (according to the experiments of V. Ya. Bezmenov and V. S. Borisov)

Theoretical curves

6.—$a = 0{\cdot}905$; $Pr_t = 0{\cdot}87$; $\rho_0/\rho_H = 20$
7.—$a = 0{\cdot}1$; $\rho_0/\rho_H = 1$
8.—$a = 0{\cdot}106$; $Pr_t = 0{\cdot}5$; $\rho_0/\rho_H = 0{\cdot}0607$.

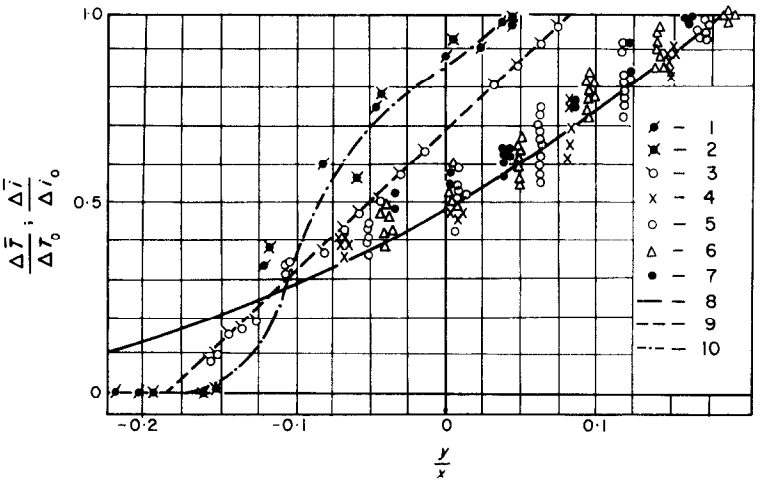

FIG. 3. Temperature (enthalpy) profiles in a boundary layer of the initial portion of cold, isothermal and hot jets.

Experimental data

Cold jet: $\Delta\bar{T}/\Delta T_0$:
1.—$x/R_0 = 10$; $T_H = 417°K$; $\rho_0/\rho_H = 20{\cdot}8$; $R_0 = 2{\cdot}5$ mm
2.—$x/R_0 = 16{\cdot}7$; $T_H = 360°K$; $\rho_0/\rho_H = 18{\cdot}8$; $R_0 = 1{\cdot}5$ mm

Isothermal jet: $\Delta\bar{T}/\Delta T_0$
3.—$x/R_0 = 2{\cdot}2$; $\rho_0/\rho_H = 1$; $R_0 = 25$ mm

Hot jet $\Delta i/\Delta i_0$:
4.—$x/R_0 = 2{\cdot}4$
5.—$x/R_0 = 3{\cdot}2$
6.—$x/R_0 = 4$
7.—$x/R_0 = 4{\cdot}8$
$\rho_0/\rho_H = 0{\cdot}00407$; $R_0 = 2{\cdot}5$ mm

Theoretical curves

8.—$a = 0{\cdot}093$; $Pr_t = 0{\cdot}87$; $\rho_0/\rho_H = 20$
9.—$a = 0{\cdot}09$; $Pr_t = 0{\cdot}5$; $\rho_0/\rho_H = 1$
10.—$a = 0{\cdot}143$; $Pr_t = 0{\cdot}5$; $\rho_0/\rho_H = 0{\cdot}00407$.

the same experimental apparatus for the same initial jet parameters we see that the temperature profiles are more full. This result also agrees with the assumption that the turbulent Prandtl number Pr_t is always less than unity for non-isothermal jets. The experimental results are compared with the theoretical results. Figures 2 and 3 give the comparison of the experimental data obtained in the initial portion of cold, isothermal and hot jets with the appropriate theoretical profiles [2, 5]. A constant a is determined as a result of comparing theoretical profiles of velocity heads, velocities, temperatures and enthalpies with the experimental ones. Its value for the initial jet portion varied from 0·09 to 0·143 and for the main portion, from 0·064 to 0·078 for the temperature variation at the nozzle outlet from 80°K to 20 × 10^3°K. At such values the theoretical profiles satisfactorily agree with the experimental data. From the data presented it is also seen that the experimental constant a somewhat increases with initial heating. This seems to indicate that the approximate theory does not take into consideration all the factors which intensify the mixing process.

In Fig. 7 is shown the change of the velocity

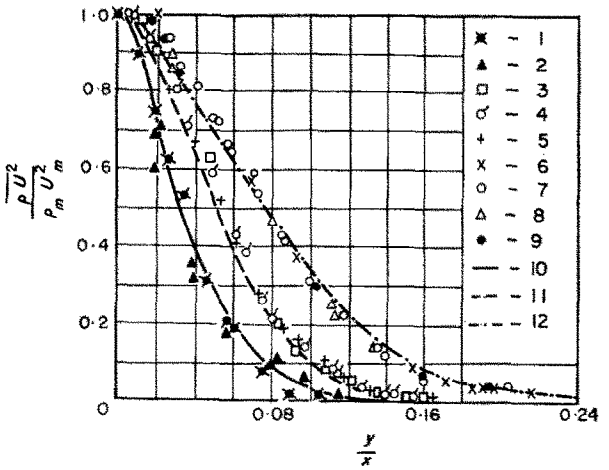

FIG. 4. Dynamic head profiles in the main portion of cold, isothermal and hot jets.

Experimental data

Cold jet:

1.—$x/R_0 = 132$; $T_H = 389°K$; $\rho_m/\rho_H = 1{\cdot}97$; $R_0 = 0{\cdot}56$ mm

2.—$x/R_0 = 92{\cdot}8$; $T_H = 408°K$; $\rho_m/\rho_H = 3{\cdot}2$; $R_0 = 0{\cdot}56$ mm

Isothermal jet:

3.—$x/R_0 = 10$
4.—$x/R_0 = 20$
5.—$x/R_0 = 30$

$\rho_0/\rho_H = 1$; $R_0 = 5$ mm

Hot jet:

6.—$x/R_0 = 16{\cdot}65$
7.—$x/R_0 = 20$
8.—$x/R_0 = 26{\cdot}6$
9.—$x/R_0 = 33{\cdot}3$

$\rho_0/\rho_H = 0{\cdot}067$; $R_0 = 15$ mm (from the experiments of V. Ya. Bezmenov and V. S. Borisov)

Theoretical curves

10.—$a = 0{\cdot}067$; $Pr_t = 0{\cdot}87$; $\rho_0/\rho_H = 20$

11.—$a = 0{\cdot}066$; $\rho_0/\rho_H = 1$

12.—$a = 0{\cdot}078$; $Pr_t = 0{\cdot}87$; $\rho_0/\rho_H = 0{\cdot}067$.

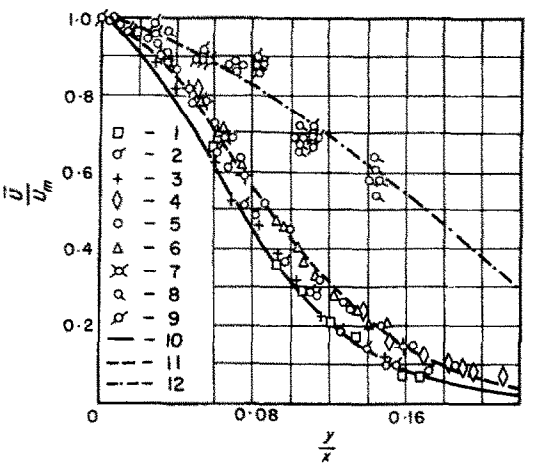

FIG. 5. Velocity profiles in the main portion of isothermal and hot jets.

Experimental data

Isothermal jet:

1.—$x/R_0 = 10$
2.—$x/R_0 = 20$
3.—$x/R_0 = 30$

$\rho_0/\rho_H = 1$; $R_0 = 5$ mm

Hot jet:

4.—$x/R_0 = 16{\cdot}65$
5.—$x/R_0 = 20$
6.—$x/R_0 = 26{\cdot}6$
7.—$x/R_0 = 33{\cdot}3$

$\rho_0/\rho_H = 0{\cdot}067$; $R_0 = 15$ mm (from the experiments of V. Ya. Bezmenov and V. S. Borisov)

8.—$x/R_0 = 7{\cdot}5$
9.—$x/R_0 = 9{\cdot}5$

$\rho_0/\rho_H = 0{\cdot}00407$; $R_0 = 7{\cdot}5$ mm

Theoretical curves

10.—$a = 0{\cdot}66$; $\rho_0/\rho_H = 1$

11.—$a = 0{\cdot}078$; $Pr_t = 0{\cdot}87$; $\rho_0/\rho_H = 0{\cdot}067$

12.—$\rho_0/\rho_H = 0{\cdot}00407$.

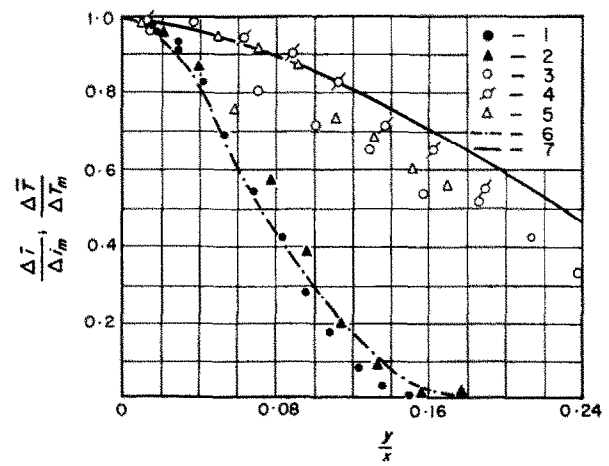

FIG. 6. Temperature and enthalpy profiles in the main portion of cold and hot jets.

Experimental data

Cold jet:

1.—$x/R_0 = 132$; $T_H = 389°K$; $\rho_m/\rho_H = 1{\cdot}97$; $R_0 = 0{\cdot}56$ mm

2.—$x/R_0 = 92{\cdot}8$; $T_H = 408°K$; $\rho_m/\rho_H = 3{\cdot}2$; $R_0 = 0{\cdot}56$ mm

Hot jet:

3.—$x/R_0 = 4{\cdot}6$;
4.—$x/R_0 = 5{\cdot}4$;
5.—$x/R_0 = 7{\cdot}4$;

$\rho_0/\rho_H = 0{\cdot}00407$; $R_0 = 7{\cdot}5$ mm

Theoretical curves

6.—$\Delta\bar{T}/\Delta T_m$; $a = 0{\cdot}064$; $Pr_t = 0{\cdot}87$

7.—$\Delta i/\Delta i_m$.

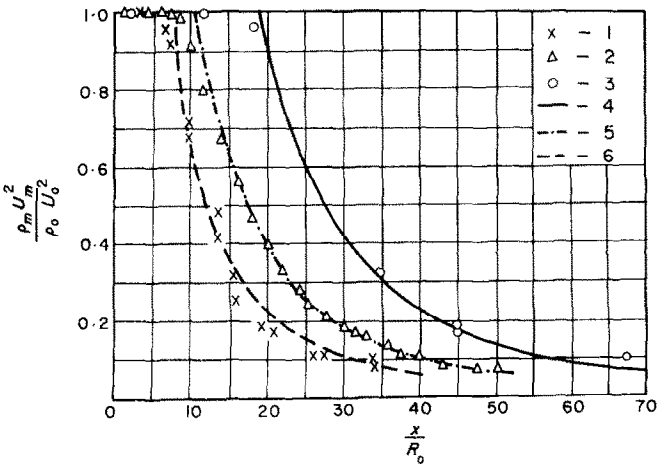

FIG. 7. Change of relative dynamic head along the axis of hot, isothermal and cold jets.

Experimental data

1.—$\rho_0/\rho_H = 0{\cdot}067$; $T_H = 280°K$; $R_0 = 15$ mm (from the experiments of V. S. Bezmenov and V. Ya. Borisov)
2.—$\rho_0/\rho_H = 1$; $R_0 = 5$ mm
3.—$\rho_0/\rho_H = 20$; $T_H = 280°K$; $R_0 = 0{\cdot}56$ mm

Theoretical curves

4.—$a = 0{\cdot}072$; $Pr_t = 0{\cdot}87$; $R_0 = 0{\cdot}56$ mm
5.—$a = 0{\cdot}075$; $R_0 = 5$ mm
6.—$a = 0{\cdot}081$; $Pr_t = 0{\cdot}87$; $R_0 = 15$ mm.

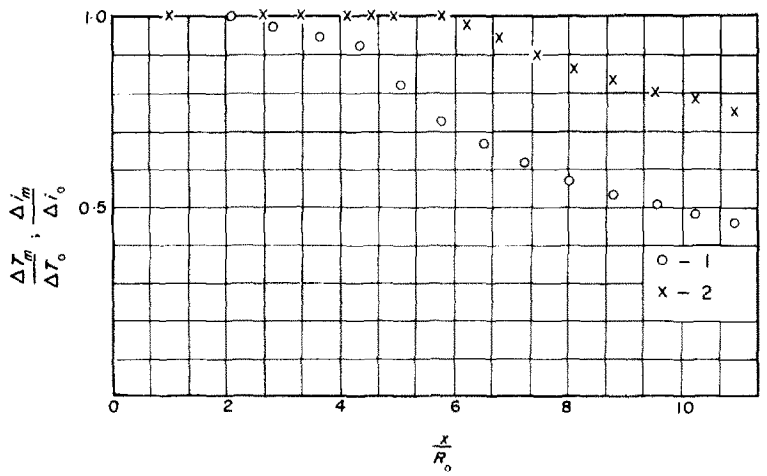

FIG. 8. Change of enthalpy along the axis of isothermal and hot jets.

Experimental data

1.—$\rho_0/\rho_H = 0{\cdot}00407$; $T_0 = 17{\cdot}5 \times 10^3°K$; $R_0 = 2{\cdot}5$ mm
2.—$\rho_0/\rho_H = 1$.

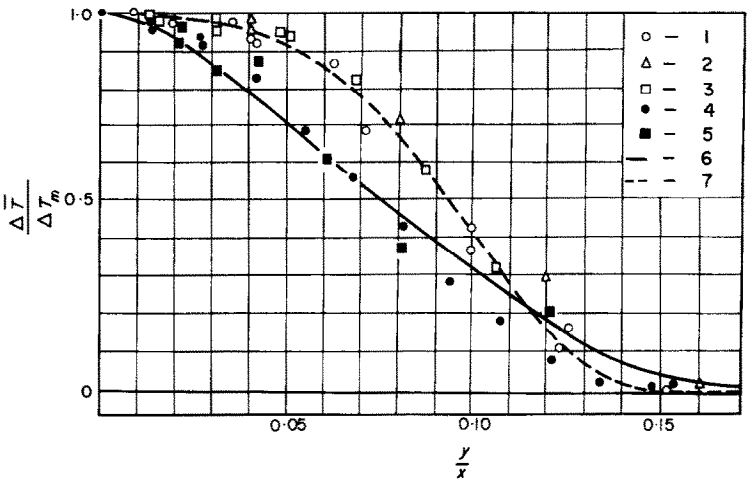

FIG. 9. Temperature profiles at different cross-sections of the main portion of a cold jet.

Experimental data

1.—$x/R_0 = 49{\cdot}4$; $T_H = 250°K$; $\rho_m/\rho_H = 8{\cdot}09$; $R_0 = 1{\cdot}5$ mm
2.—$x/R_0 = 44{\cdot}6$; $T_H = 282°K$; $\rho_m/\rho_H = 7{\cdot}84$; $R_0 = 0{\cdot}56$ mm
3.—$x/R_0 = 34{\cdot}7$; $T_H = 287°K$; $\rho_m/\rho_H = 10{\cdot}4$; $R_0 = 1{\cdot}5$ mm
4.—$x/R_0 = 132$; $T_H = 389°K$; $\rho_m/\rho_H = 1{\cdot}97$; $R_0 = 0{\cdot}56$ mm
5.—$x/R_0 = 66{\cdot}7$; $T_H = 200°K$: $\rho_m/\rho_H = 2{\cdot}71$; $R_0 = 1{\cdot}5$ mm

Theoretical curves

6.—$a = 0{\cdot}064$; $Pr_t = 0{\cdot}87$; $\rho_m/\rho_H = 2{\cdot}5$.
7.—$a = 0{\cdot}0665$; $Pr_t = 0{\cdot}87$; $\rho_m/\rho_H = 8{\cdot}0$.

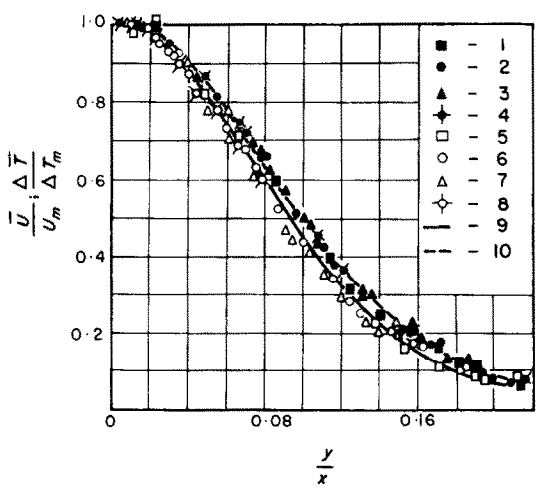

FIG. 10. Velocity and temperature profiles in the main portion of a hot jet (from the experiments of V. Ya. Bezmenov and V. S. Borisov).

Experimental data

1.—$x/R_0 = 16{\cdot}65$
2.—$x/R_0 = 20$
3.—$x/R_0 = 26{\cdot}6$
4.—$x/R_0 = 33{\cdot}3$
} $\Delta\bar{T}/\Delta T_m$; $\rho_0/\rho_H = 0{\cdot}067$; $R_0 = 15$ mm

5.—$x/R_0 = 16{\cdot}65$
6.—$x/R_0 = 20$
7.—$x/R_0 = 26{\cdot}6$
8.—$x/R_0 = 33{\cdot}3$
} $\bar{u}/u_m$; $\rho_0/\rho_H = 0{\cdot}067$; $R_0 = 15$ mm

Theoretical curves

9.—$a = 0{\cdot}078$; $Pr_t = 0{\cdot}87$; $\bar{u}/u_m$
10.—$a = 0{\cdot}076$; $Pr_t = 0{\cdot}87$; $\Delta\bar{T}/\Delta T_m$.

head on the axes of cold, isothermal and hot jets at $T_0 = 4000°K$,† and also the comparison of the theoretical and experimental results which are in good agreement ($a = 0{\cdot}072$–$0{\cdot}081$). These values of the constant a are close to its values determined by comparing the appropriate cross-sectional experimental and theoretical profiles. Finally it may be said that the semi-empirical theories of turbulence used as the base of the calculation of non-isothermal jets, satisfactorily agree with the experimental data when a comparatively slight change is made of the empirical constant.

CONCLUSIONS

The present paper gives the results of a theoretical and experimental investigation of jets over a wide range of change of the initial density ratio ρ_0/ρ_H (or a temperature ratio T_0/T_H). The experimental investigations have shown that the expansion angles of a jet as well as the profile configuration mainly depend upon the initial density ratio.

The methods for calculating such non-isothermal jets satisfactorily agree with the available experimental data with a change of the experimental constant a over a comparatively small range.

†Data on a hot jet with $T_0 = 4000$ °K are taken from the experiments by V. Ya. Bezmenov and V. S. Borisov.

REFERENCES

1. G. N. ABRAMOVICH, *Turbulent Jet Theory*. Fitzmatgiz, Moscow (1960).
2. V. I. BAKULEV, Calculation of a turbulent submerged real gas jet, *Inzh. Zh.* **1**, vyp, 3, 65–75 (1961).
3. V. A. GOLUBEV, A theoretical investigation of a turbulent plane parallel stream at high temperature with calculation of dissociation and ionization. *Inzh. Fiz. Zh.* **7** (10), 42–50 (1961).
4. V. A. GOLUBEV, On calculation of turbulent jet flow at very high temperature. *Inzh. Zh.* **1**, vyp. 4, 5158 (1961).
5. V. I. BAKULEV, Calculation of the main portion of an axisymmetric turbulent real gas jet. *Inzh. Fiz. Zh.* **7** (10), 14–20 (1964).
6. V. A. GOLUBEV, YU. V. MOSKVIN and S. K. KHOVRIN, *Teplofiz. Vysok. Temper.* **3** (5), 669–676 (1965).

Abstract—The present paper is devoted to the theoretical and experimental study of submerged non-isothermal turbulent jets in a temperature range from 50–100°K to 20×10^3 °K.

Résumé—L'article est consacré à l'étude théorique et expérimentale de jets turbulents submergés non isothermes dans la gamme de températures initiales allant de 50 à 100°K jusqu'à 20×10^3°K.

Zusammenfassung—Die vorliegende Arbeit befasst sich mit der theoretischen und experimentellen Untersuchung eines nichtisothermen Strahls im Temperaturbereich von 50–100°K bis 20×10^3°K.